Journal of Chemistry and Technologies, 2026, *34*(1), 266-272

Journal of Chemistry and Technologies

pISSN 2663-2934 (Print), ISSN 2663-2942 (Online).

journal homepage: http://chemistry.dnu.dp.ua
editorial e-mail: chem.dnu@gmail.com

UDC 621.318.1: **546.05**

EFFECT Of OH^-/M^{2+} RATIO ON THE PROPERTIES OF $Fe/CoFe_2O_4$ COMPOSITES OBTAINED BY HYDROTHERMAL METHOD

Liliya A. Frolova[1], Dmytro Yu. Saltykov[2], Iryna V. Sknar[1]

[1]*Ukrainian State University of Science and Technologies, 8 Nauky Ave., Dnipro, 49005, Ukraine*
[2]*Oles Honchar Dnipro National University, 72 Nauky Ave., Dnipro, 49010, Ukraine*

Received 6 October 2025; accepted 28 January 2026; available online 23 March 2026

Abstract

Nanodisperse composites were synthesized by hydrothermal method at elevated pressure. To study the influence of OH^-/M^{2+} concentration ratio on phase composition, degree of crystallinity, average crystallite size, magnetic and absorption properties of $Fe/CoFe_2O_4$ composites, a series of $Fe/CoFe_2O_4$ composites was obtained by varying synthesis conditions. The obtained composites were characterized by X-ray diffraction, scanning electron microscopy, vibrational magnetometry and microwave analysis. A larger excess of precipitant leads to a higher degree of crystallinity and a larger average crystallite size of $CoFe_2O_4$. With an increase in the [OH^-/Me^{2+}] ratio, the diffraction peaks significantly increase in sharpness and intensity, indicating the formation of crystals with higher crystallinity and average crystallite size. Noticeable shifts in the positions of the diffraction peaks are also found for all samples, while the value of the crystal lattice constant decreases (8.3901–8.3699 Å). Studies using vibrational magnetometry have shown that the dependence of the saturation magnetization (M_s) correlates with the α-Fe content. The maximum values of the saturation magnetization of 200 Emu/g and the coercive force of 900 Oe correspond to a ratio of OH^-/M^{2+} concentrations equal to 4.6. All obtained samples effectively absorb electromagnetic radiation in the range of 8–10 GHz.

Keywords: magnetic properties; spinel; X-ray phase analysis.

ВПЛИВ СПІВВІДНОШЕННЯ OH^-/M^{2+} НА ВЛАСТИВОСТІ КОМПОЗИТІВ $Fe/CoFe_2O_4$, ОТРИМАНИХ ГІДРОТЕРМАЛЬНИМ МЕТОДОМ

Лілія А. Фролова[1], Дмитро Ю. Салтиков[2], Ірина В. Скнар[1]

[1]*Український державний університет науки і технологій, , просп.Науки, 8, Дніпро,49005, Україна*
[2]*Дніпровський національний університет імені Олеся Гончара, просп. Науки, 72, Дніпро, 49010, Україна*

Анотація

Нанодисперсні композити були синтезовані гідротермальним методом за підвищеного тиску. Для вивчення впливу співвідношення концентрацій OH^-/M^{2+} на фазовий склад, ступінь кристалічності, середній розмір кристалітів, магнітні та абсорбційні властивості композитів $Fe/CoFe_2O_4$ було отримано серію композитів $Fe/CoFe_2O_4$ шляхом варіювання умов синтезу. Отримані композити були охарактеризовані за допомогою рентгенівської дифракції, скануючої електронної мікроскопії, коливальної магнітометрії та мікрохвильового аналізу. Більший надлишок осаджувача призводить до вищого ступеня кристалічності та більшого середнього розміру кристалітів $CoFe_2O_4$. Дослідження з використанням коливальної магнітометрії показали, що залежність намагніченості насичення (Ms) корелює з вмістом α-Fe. Розміри нанокристалів композиту $Fe/CoFe_2O_4$, розраховані за формулою Шеррера, коливалися від 93.5 до 123.4 нм. Максимальні значення намагніченості насичення 200 А $м^2$/кг та коерцитивної сили 900 Ерстед відповідають значенню n = 4.6.

Ключові слова: магнітні властивості; шпінель; рентгенофазовий аналіз.

**Corresponding author: e-mail: domosedi@i.ua*

doi: 10.15421/jchemtech.v34i1.332246

Journal of Chemistry and Technologies, 2026, *34*(1), 266-272

Introduction

Nanosized transition metal ferrites with spinel structure have recently attracted wide attention of researchers in various scientific and applied fields [1–3]. Cobalt ferrite $CoFe_2O_4$, one of the well-known magnetically hard materials, is widely used as a high-density recording medium, photocatalysts, adsorbents, electromagnetic radiation absorbers due to its significant magnetic anisotropy, moderate saturation magnetization, and high coercivity [4]. To date, there are a number of technologies that have been previously described for the preparation of $CoFe_2O_4$ nanocrystals, including plasma, ultrasound, microemulsion, sol-gel methods, coprecipitation, electrochemical synthesis [5–10]. Ceramic high-temperature method is the most widely used method due to its high productivity and simplicity in the production of magnetic materials [11]. However, the inability to obtain nanodispersed and monodispersed products limits its use despite the high productivity. To date, there are many hydrothermal synthesis methods used to produce $CoFe_2O_4$ nanocrystals, which differ in synthesis temperature, pressure, and precursors [12–14]. Detailed studies have reported the preparation of $CoFe_2O_4$ nanocrystals by mixing 0.2 M $Fe(NO_3)_3$, 0.1 M $Co(NO_3)_2$ and 6 M NaOH [15; 16]. In this case, no additional oxidizer is required to form $CoFe_2O_4$. Previous studies have also shown that precursors and synthesis temperature play an important role in controlling the size of $CoFe_2O_4$, which significantly affects the phase composition and functional properties of the products [17; 18]. Very often, attempts are made to improve the magnetic properties of $CoFe_2O_4$ nanocrystals by increasing the calcination temperature of coprecipitated compounds or oxides [19; 20]. In the present study, nanodispersed $Fe/CoFe_2O_4$ composites were obtained using the hydrothermal method. The aim of this study is to investigate the effect of the metal cation/alkali molar ratio on the crystallite size, crystallinity, magnetic properties and phase composition of the resulting products. A series of $Fe/CoFe_2O_4$ samples with different crystallite sizes and crystallinity were prepared by varying not only the pH but also the excess alkali during the synthesis. To our knowledge, these aspects have not been considered in detail in previous studies.

Experimental

Aqueous solutions of cobalt sulfate and iron sulfate were used as starting materials. The nanosized composite was prepared in a hydrothermal reactor.

Four samples with different [OH^- /Me^{2+}] ratios were synthesized.

Table 1.

Conditions for sample synthesis

№ sample	Ratio [OH^- / Me^{2+}]
1	2.0
2	2.1
3	3.3
4	4.6

The obtained product was washed and dried for further study. The phase composition and structure of the ferrite samples were studied using a DRON-2 X-ray diffractometer with Co-Kα r The crystallite sizes were determined by the Selyakov-Scherrer formula.

$$L_{HKL} = \frac{0.94\lambda}{\beta Cos\theta_{HKL}}, \quad (1)$$

where λ is a wavelength of radiation;

β is a half-width of the reflection line;

θ is a maximum angle;

L_{HKL} is a crystallite size in the direction of reflection (HKL).

The value of microstresses is determined by the formula:

$$\boldsymbol{M} = \frac{\boldsymbol{\Delta d}}{\boldsymbol{d}} = \frac{\boldsymbol{\Delta a}}{\boldsymbol{a}} = \frac{\boldsymbol{\beta}}{\boldsymbol{4tg\theta_{HKL}}}, \quad (2)$$

M – degree of microstresses'

M is determined by solving two equations with two unknowns.

D_{nkl} is- dislocation density in the direction (HKL).

$$D_{HKL} = A\beta^2, \quad (3)$$

where A is coefficient depending on the elastic properties of materials.

Lattice paramete adiation.

$$a = \sqrt{(H^2 + K^2 + L^2)} \quad (4)$$

The magnetic properties of the final powder were studied using a vibration magnetometer. Measurements of the complex absorption and reflection coefficient, reflection coefficient, specific absorption for ferrites were performed using a setup consisting of a G4-83 generator, a S4–11 spectrum analyzer, and a biconical resonator. The measurements were performed at a frequency of 10^8–10^{12} Hz at a temperature of 20 °C. The thickness of the sample was 1 mm.

Results and discussion

The diffraction patterns of the obtained $Fe/CoFe_2O_4$ samples are shown in Fig. 1.

Journal of Chemistry and Technologies, 2026, *34*(1), 266-272

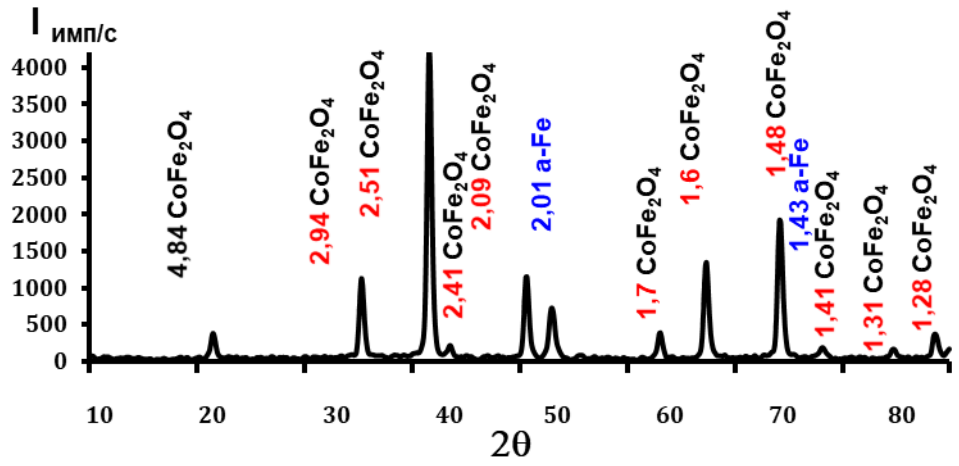

a

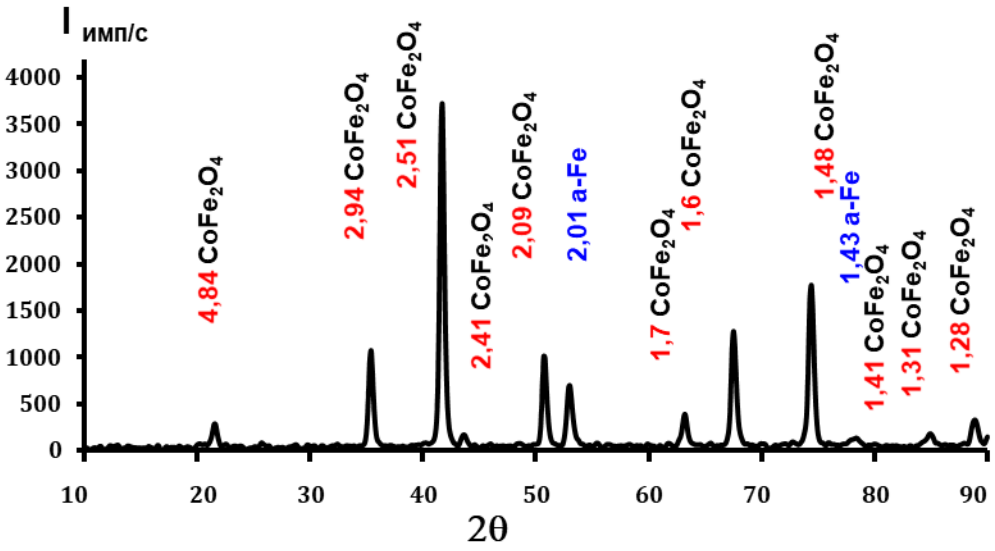

b

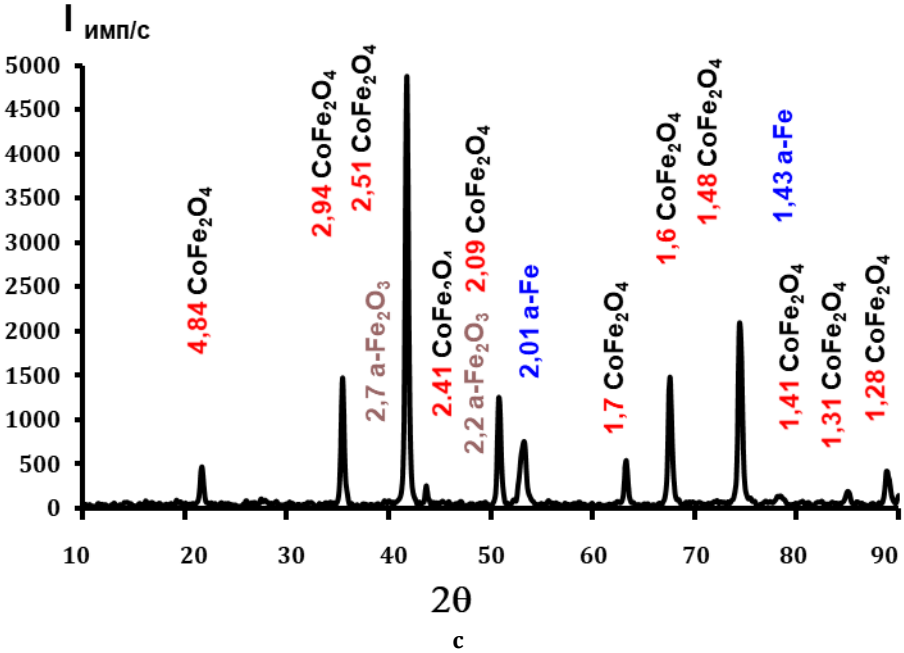

c

Journal of Chemistry and Technologies, 2026, *34*(1), 266-272

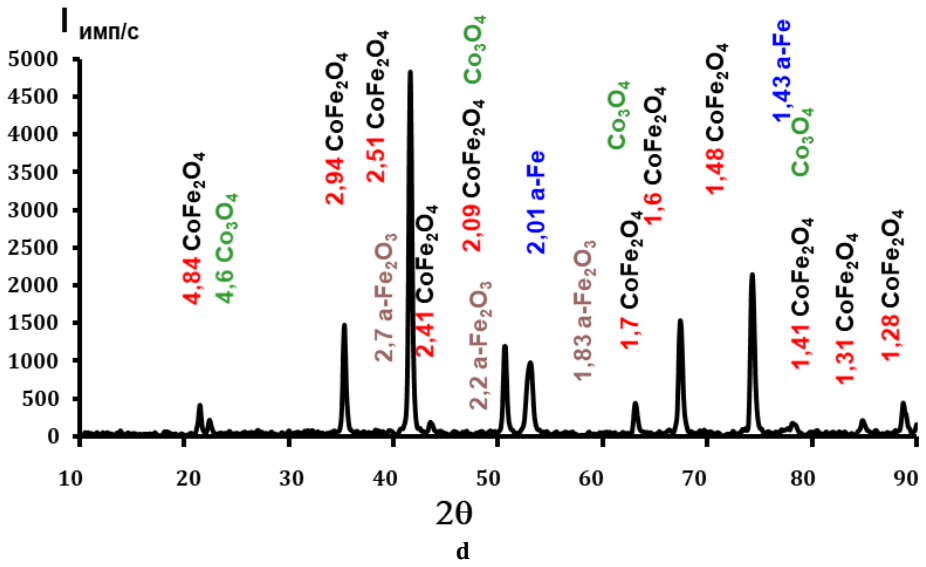

Fig. 1. X-ray diffraction patterns of the synthesized samples (numbering in accordance with Table 1)

The X-ray diffraction patterns confirm the formation of a composite consisting of spinel ferrite $CoFe_2O_4$ with a cubic lattice (coincides with the standard X-ray diffraction pattern (JCPDS card No. 22-1086) and alpha iron. Additional impurities in the form of Co_3O_4, α-$_{Fe2O3}$, appear in sample 4. No impurities were found in sample 1, 2 and 3.

Table 2

Structural characteristics of the samples

	Sample 1	Sample 2	Sample 3	Sample 4
a, A	8.3901	8.3843	8.3795	8.3698
Phase composition	$CoFe_2O_4$ (F-43m cubic syngony) α-Fe	$CoFe_2O_4$ (F-43m cubic syngony) α-Fe	$CoFe_2O_4$ (F-43m cubic syngony) α-Fe	$CoFe_2O_4$ (F-43m cubic syngony), Co_3O_4, α-Fe_2O_3 α-Fe
degree of micro stress M	$1.01 \cdot 10^{-4}$	$0.42 \cdot 10^{-4}$	$1.475 \cdot 10^{-4}$	$1.475 \cdot 10^{-4}$
L_{311} A	937	1002	1006	1179
L_{440} A	1041	1145	1314	1234
L A	1046	1252	1256	1474
D_{311} cm^{-2}	$10.45 \cdot 10^{10}$	$7.29 * 10^{10}$	$7.23 \cdot 10^{10}$	$5.39 \cdot 10^{10}$
D_{440} cm^{-2}	$9.21 \cdot 10^{10}$	$7.7 * 10^{10}$	$5.85 \cdot 10^{10}$	$6.33 \cdot 10^{10}$
$I^{CoFe2O4}{}_p$/ $I^{Fe}{}_p$, abs.un.	4251/673	3717/695	4867/729	4826/979
ϖ(Fe), %	64.8	65.4	70.1	67.8

Table 2 also shows an obvious increase in crystallinity with increasing molar ratio. The intensity ($I_{CoFe2O4p}/I_{Fep}$) of both ferrite and alpha iron peaks increases significantly with increasing [OH- /Me^{2+}] value. The average crystallite size (L_{311}) of the nanocrystals increases from 93.5 to 117.9 nm with increasing n from 2 to 4.6. It can be clearly seen that with increasing [OH^- /Me^{2+}] ratio, the diffraction peaks increase significantly in sharpness and intensity, suggesting the formation of crystals with higher crystallinity and average crystallite size. The calculated L_{440} value of $CoFe_2O_4$ nanocrystals also increases from 104.0 to 147.4 nm with increasing molar ratio. Noticeable shifts in the position of the diffraction peaks are also found for all the samples, with the lattice constant value decreasing (8.3901–8.3699 Å). The morphology of sample 1 is shown in Fig. 2. The size of the crystallites was determined using electron microscopy (Fig. 2), showing that the average physical size of the Fe/$CoFe_2O_4$ nanocomposites for sample 1 is 150–200 nm, which is slightly larger than the crystallite size determined from the X-ray diffraction patterns due to the agglomeration of primary particles.

Journal of Chemistry and Technologies, 2026, *34*(1), 266-272

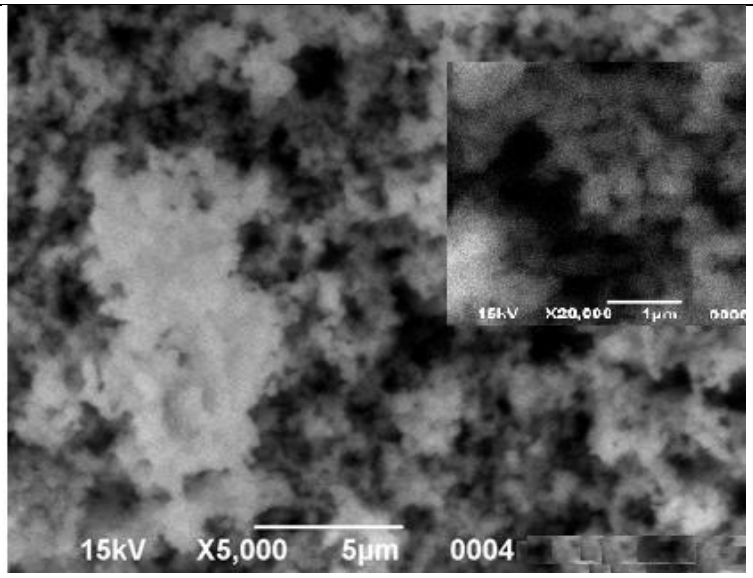

Fig. 2. SEM images of synthesized products

As can be seen, the particles of $Fe/CoFe_2O_4$ nanocomposites obtained at the stoichiometric ratio have a clearly defined spherical shape.

Magnetic hysteresis loops M=f(H) for $Fe/CoFe_2O_4$ nanocomposites are shown in Fig. 3(a, b). A detailed look at Fig. 3(a) shows the correlation between the coercive force (Hc) and the composite composition. Since the average size of $CoFe_2O_4$ crystallites in two planes increases with increasing n, the coercive force Hc of the composite increased with increasing L_{311} and L_{440}. This increase is due to a higher degree of crystallinity. In addition, excess alkali promotes both the redistribution of Co^{2+} and Fe^{3+} ions located in octahedral and tetrahedral sites and the formation of additional phases. The maximum values of saturation magnetization 200 Em/kg and coercive force 900 Oersted correspond to n = 4.6.

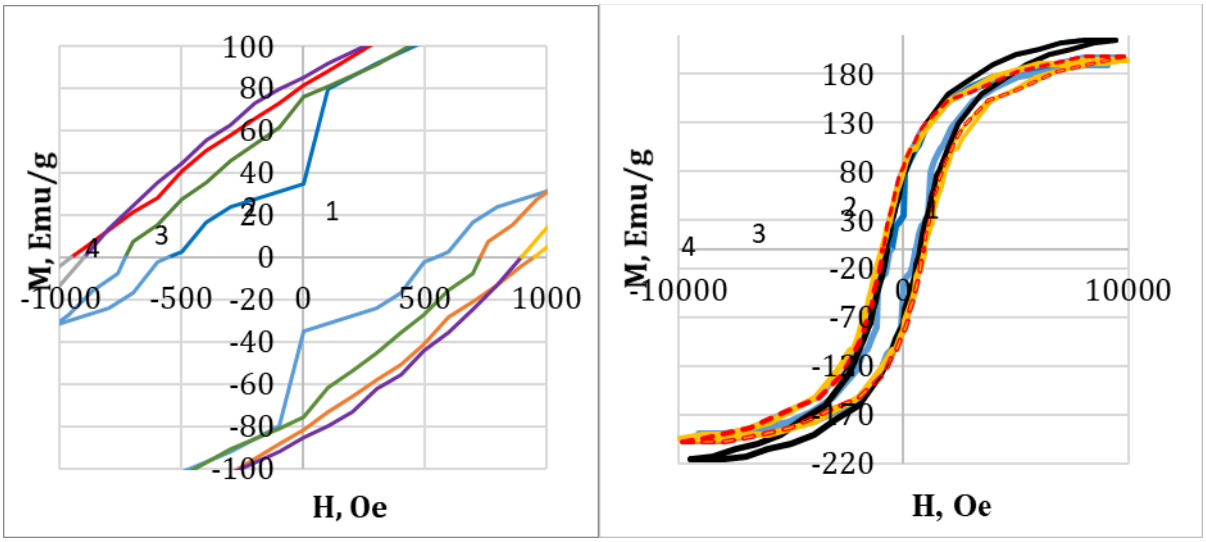

Fig. 3. Hysteresis loops (a) and a fragment of a hysteresis loop (b)

In addition, the Hc of the $Fe/CoFe_2O_4$ composite was studied as a function of the crystallite size. Figure 4 shows an increase in Hc (560–920 Oe) with increasing alkali/metal ratio for samples 1–2. Hc then decreased slightly to 850 Oe with increasing ϖ(Fe). The saturation magnetization increased monotonically with increasing ϖ(Fe), which correlates with increasing proportion of iron in the composite.

Journal of Chemistry and Technologies, 2026, *34*(1), 266-272

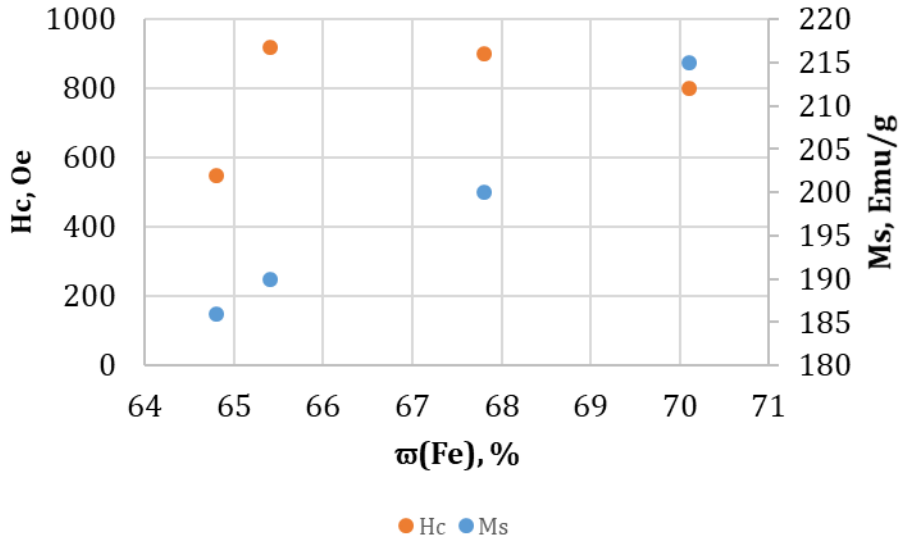

Fig. 4. Dependence of the magnitude of the coercive force, residual magnetization and saturation magnetization on the ratio [OH^- /Me^{2+}]

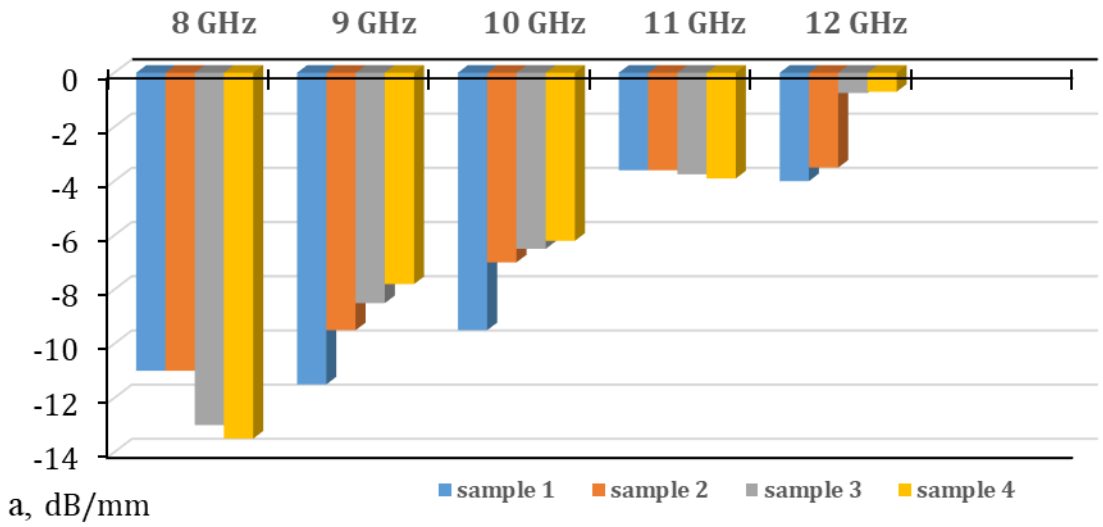

Fig. 5. Dependence of the specific absorption of electromagnetic radiation on the frequency for samples 1-4

As can be seen from Figure 5, all the obtained samples effectively absorb EMR in the range of 8–10 GHz. In this case, the highest values of 14 dB/mm correspond to sample 4. At a frequency of 9–12 GHz, the highest values correspond to sample 1.

Conclusions

In this work, the Fe/$CoFe_2O_4$ nanocrystalline composite was obtained using the hydrothermal method. The degree of crystallinity and the average crystallite size of the Fe/$CoFe_2O_4$ nanocrystals are controlled by changing the [OH^- /Me^{2+}] ratio. Higher values led to a higher degree of crystallinity and a larger average crystallite size of the Fe/$CoFe_2O_4$ nanocrystals and an increase in the iron content. The results show that the magnetic properties (Ms, Hc) of the Fe/$CoFe_2O_4$ composite nanocrystals increased significantly with an increase in the average crystallite size. The sizes of Fe/$CoFe_2O_4$ composite nanocrystals, calculated using the Scherrer formula, ranged from 93.5 to 123.4 nm. The maximum values of saturation magnetization ~200 Emu/g and coercive force 900 Oersted correspond to a value of n = 4.6.

References

[1] Arora, K., Ledwani, L., & Komal, Dr. (2025). A Comprehensive Review on the Synthesis and Therapeutic Potential of Cobalt Ferrite ($CoFe_2O_4$) Nanoparticles. *Chemistry Select*, *10*(1), e202404136. https://doi.org/10.1002/slct.202404136

[2] Chamaraja, N. A., Swamy, N. K., Shivakumar, V., Kavya, H. V., & Bvaraju, M. (2025). Evaluation of

peroxidase mimetic properties of cobalt ferrite ($CoFe_2O_4$) nanoparticles and their applications in the assay of aminophenols in water samples. *Nanotechnology for Environmental Engineering, 10*(1), 15. doi:10.1007/s41204-025-00413-z

[3] Patil, P. S., Bhagat, S., Kokate, R., & Jadhav, K. M. (2025). Investigations of structural, optical and magnetic properties of $CoFe_2O_4$ nano-catalyst for hydrogen production applications. *In AIP Conference Proceedings*, *3198*(1), 020032. https://doi.org/10.1063/5.0248275

[4] Jasrotia, R., Prakash, J., Saddeek, Y. B., Alluhayb, A. H., Younis, A. M., Lakshmaiya, N., Prakash, C., Aly K.A., Sillanpa M., Ismail, Y., Kandwal, A., & Sharma, P. (2025). Cobalt ferrites: Structural insights with potential applications in magnetics, dielectrics, and Catalysis. *Coordination Chemistry Reviews*, *522*, 216198. doi:10.1016/j.ccr.2024.216198

[5] Ismail, M., Ali, N. A., Sazelee, N. A., Muhamad, S. U., Suwarno, S., & Idris, N. H. (2022). $CoFe_2O_4$ synthesized via a solvothermal method for improved dehydrogenation of $NaAlH_4$. *International Journal of Hydrogen Energy*, 47(97), 41320–41328. https://doi.org/10.1016/j.ijhydene.2022.01.215

[6] Bayça, F. (2024). Characterization and magnetic properties of $CoFe_2O_4$ nanoparticles synthesized by the co-precipitation method. *International Journal of Applied Ceramic Technology*, *21*(1), 544-554. https://doi.org/10.1111/ijac.14518

[7] Gingasu, D., Culita, D. C., Calderon Moreno, J. M., Marinescu, G., Bartha, C., Oprea, O., Preda, S., Chifiriuc, M. C., & Popa, M. (2023). Synthesis of $CoFe_2O_4$ through wet ferritization method using an aqueous extract of eucalyptus leaves. *Coatings*, *13*(7), 1250. https://doi.org/10.3390/coatings13071250

[8] Heydaryan, K., Kashi, M. A., & Montazer, A. H. (2022). Tuning specific loss power of $CoFe_2O_4$ nanoparticles by changing surfactant concentration in a combined co-precipitation and thermal decomposition method. *Ceramics International*, *48*(12), 16967–16976. doi:10.1016/j.ceramint.2022.02.251

[9] Vishwas, M., Babu, K. V., Gowda, K. A., & Gandla, S. B. (2022). Synthesis, characterization and photo-catalytic activity of magnetic $CoFe_2O_4$ nanoparticles prepared by temperature controlled co-precipitation method. *Materials Today: Proceedings*, *68*(11), 497–501. doi:10.1016/j.matpr.2022.07.429

[10] Boussafel, H., Sedrati, C., & Alleg, S. (2024). Green synthesis of $NiFe_2O_4$, $CoFe_2O_4$, and NiO. $5CoO.5Fe_2O_4$ by sol–gel autocombustion method using olive leaf extract as fuel. *Applied Physics A*, *130*(6), 374. doi:10.1007/s00339-024-07547-y

[11] Shakirzyanov, R. I., Kozlovskiy, A. L., Zdorovets, M. V., Zheludkevich, A. L., Shlimas, D. I., Abmiotka, N. V., Kazantsev, P.A., Zubar, T.I., Trukhanov, S. V., & Trukhanov, A. V. (2023). Impact of thermobaric conditions on phase content, magnetic and electrical properties of the $CoFe_2O_4$ ceramics. *Journal of Alloys and Compounds*, 954, 170083. https://doi.org/10.1016/j.jallcom.2023.170083

[12] Huang, T., Qiu, Z., Hu, Z., & Lu, X. (2021). Novel method of preparing hierarchical porous $CoFe_2O_4$ by the citric acid-assisted sol-gel auto-combustion for supercapacitors. *Journal of Energy Storage*, *35*, 102286. https://doi.org/10.1016/j.est.2021.102286

[13] Ravindra, A. V., & Ju, S. (2023). Mesoporous $CoFe_2O_4$ nanocrystals: Rapid microwave-hydrothermal synthesis and effect of synthesis temperature on properties. *Materials Chemistry and Physics*, *303*, 127818. https://doi.org/10.1016/j.matchemphys.2023.127818

[14] Prasad, K., Sreekanth, T. V. M., Yoo, K., & Kim, J. (2023). Surfactant-assisted hydrothermal synthesis of CoFe2O4 nanostructures and their application in the oxygen evolution reaction. *Materials Letters*, *349*, 134859. doi:10.1016/j.matlet.2023.134859

[15] Xiangfeng, C., Dongli, J., Yu, G., & Chenmou, Z. (2006). Ethanol gas sensor based on $CoFe_2O_4$ nano-crystallines prepared by hydrothermal method. *Sensors and Actuators B: Chemical*, *120*(1), 177–181. doi:10.1016/j.snb.2006.02.008

[16] Zhao, D., Wu, X., Guan, H., & Han, E. (2007). Study on supercritical hydrothermal synthesis of $CoFe_2O_4$ nanoparticles. *The Journal of supercritical fluids*, 42(2), 226–233. doi:10.1016/j.supflu.2007.03.004

[17] Ansari, S. M., Younis, A., Kolekar, Y. D., & Ramana, C. V. (2025). Cobalt ferrite nanoparticles: The physics, synthesis, properties, and applications. *Applied Physics Reviews*, 12(2), 021308. https://doi.org/10.1063/5.0244555

[18] Tatarchuk, T., Shyichuk, A., Kotsyubynsky, V., & Danyliuk, N. (2025). Catalytically active cobalt ferrites synthesized using plant extracts: Insights into structural, optical, and catalytic properties. *Ceramics International*, *51*(4), 4988–4999. https://doi.org/10.1016/j.ceramint.2024.11.470

[19] Yadav, S. M., Kumar, S., Kumar, M., Ghosh, A., & Saini, D. S. (2024). High-temperature variable range hopping conduction and dielectric relaxation in $CoFe_2O_4$ ceramic. *Open Ceramics*, *17*, 100517. https://doi.org/10.1016/j.oceram.2023.100517

[20] Varma, P. R., Manna, R. S., Banerjee, D., Varma, M. R., Suresh, K. G., & Nigam, A. K. (2008). Magnetic properties of $CoFe_2O_4$ synthesized by solid state, citrate precursor and polymerized complex methods: A comparative study. *Journal of Alloys and Compounds*, *453*(1-2), 298–303. DOI:10.1016/j.jallcom.2006.11.058